RESEARCH OF PROTECTIVE PROPERTY AIRCRAFT STRUCTURE UNDER UNCONTAINED ENGINE DEBRIS IMPACT

Andrey V. Chernov*
***Central Aero-Hidrodynamic Institute (TsAGI), Zhukovsky, Moscow Region, Russia**

Keywords: *Engine debris, Impact, Numerical Methods*

Abstract

For commercial aircrafts engine debris impact poses one of the most dangerous threats to a safe flight. This risks were shown in airworthiness regulation documentation (FAR, JAR, AP and other) of all countries of the world. The paper presents the numerical simulation process verification of engine debris impact on aircraft structure by using well known real test results. Sensitivity studies were carried out to assess the influence geometrical parameters such as the struck aircraft structures dimensions, the thickness, as well as impact parameters, projectile size and velocity, impact angle, boundary conditions. A detailed nonlinear transient finite element analysis was carried out using an explicit FE code, continuing a research approach on these topics, these results allowed to provide possible guidelines for future protective structure design.

1 Introduction

Although the conditions of aircraft engine rotors are regularly monitored, uncontained disk burst events still occur worldwide. Uncontained rotor failures can be caused by various reasons including fatigue and internal and external foreign object debris. These projectiles can strike not only airframe structure but also the passengers, the hydraulic control system components, the neighboring engines, the fuel tanks etc. The impressive examples of this it are the accidents which happened with DC-10 3rd of November 1973 (fig. 1) [1] and with DC-10-10 19th June 1989 (fig. 2) [2].

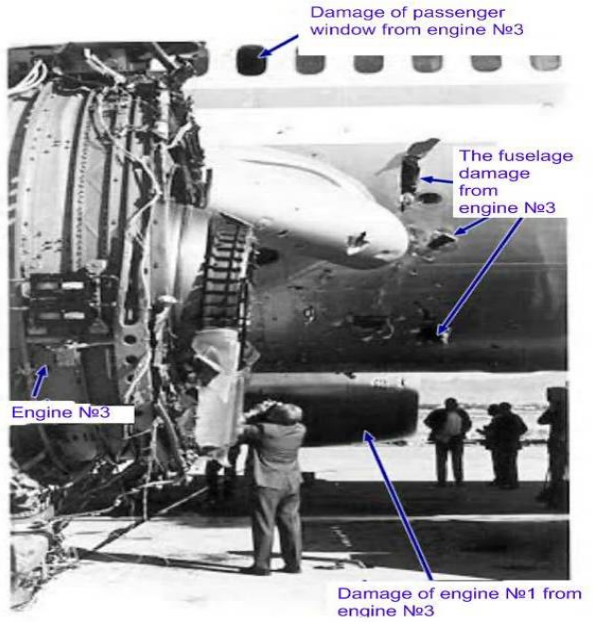

Fig. 1. The example of uncontained engine debris failure which happened with DC-10 3rd of November 1973

Fig. 2. The example of uncontained engine debris failure which happened with DC-10-10 19th June 1989

Nowadays configurations of aircrafts with package engine installation become more and more popular. Such types of planes have a number of aerodynamic and ecological advantages in comparison with planes of the

traditional scheme. But in this case there is a damage probability of the engine by fragments of the neighboring engine in case of its destruction. In frame of this paper protective property aircraft structure and protective shield design are considered.

2 Computational Modeling and Verification of Engine Debris Impact Process in Frame of MSC.Dytran Code

MSC.Dytran is a three-dimensional analysis code for analyzing the dynamic, nonlinear behavior of solid components, structures, and fluids. It uses explicit time integration and incorporates features that simulate a wide range of material and geometric nonlinearity [3].

The verification of the MSC.Dytran numerical simulation of impact process of the small engine fragments was performed with use of the well known experimental results taken from the literature references. The various forms of the projectiles (a sphere, a parallelepiped, a cylinder) were considered. For example the results of the numerical simulation of the small engine fragment impact are shown in fig. 2. The weight of a titan fragment was 25 grams and the thickness of the fuselage skin was 1mm. The results of this experiment are taken from reference [4]

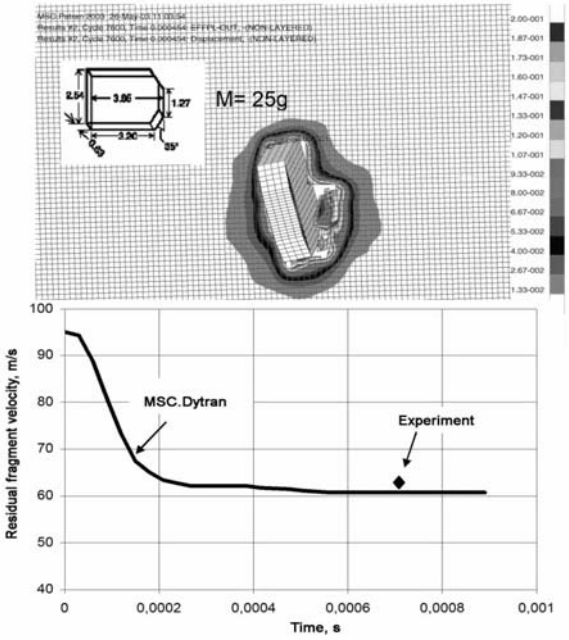

Fig. 3. Numerical simulation of small engine debris impact

According to results of the experiment the residual velocity of the projectile is equal 61.8 m/s. According to results of the numerical simulation the residual velocity of the projectile is equal 61 m/s (see Fig. 4).

In frame of NACRE program Task 3.2.3 real tests of engine debris impact with kinetic energy up to 150 kJ are performed [5]. Experiments took place in FKP GkNIPAS enterprise field. Object of research is a protective screen. It is installed on the carriage and accelerated by rocket engine along railway track (see Fig. 4). The engine fragment is fixed on special support.

Such kind of tests allows for consider impact of the big weight engine fragments with high kinetic energy and for provide the fixed initial position relative a target.

Fig. 4. General view of the test bench

The result of the 6.7 kg fragment impact on an aluminum plate (2024T351) with 40 mm thickness is shown in Fig. 5. The initial velocity of carriage was 214 m/s.

Fig. 5. The result of the 6.7 kg fragment impact

There was a perforation of the plate and full braking of a fragment (the residual speed of a fragment is equal 0 m/s). The energy absorbed by a plate is equal 153.41 kJ.

The results of numerical simulation by using MSC.Dytran code are shown in Fig. 6.

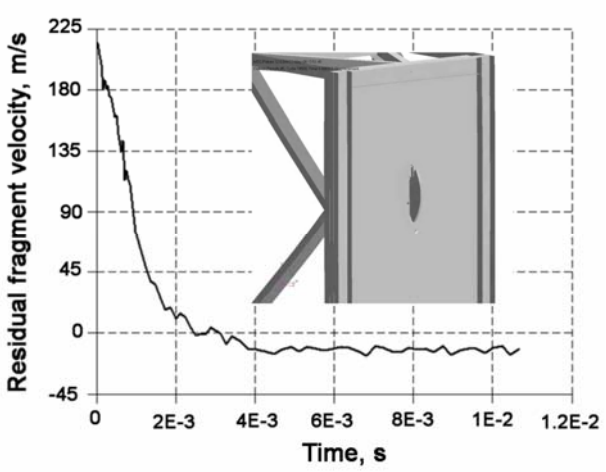

Fig. 5. The result of numerical simulation of the 6.7 kg fragment impact

According to results of numerical simulation there is a perforating of the plate and rebound of the fragment (residual velocity of the fragment is equal 10 m/s). The energy absorbed by a plate is equal 153.08 kJ. According to results of the experiment the energy absorbed by a plate is equal 153.41 kJ, i.e. they practically coincide.

3 Numerical Parametrical Researches

The engineering method is based on the experience of numerous results of numerical impact simulations in frame of MSC.Dytran code.

A characteristic of protective properties of a structure is an energy absorbed by structure $E_{absorbed}$.

The following varied parameters were chosen:

E_{debris} - kinetic energy of the fragment,

t - the plate thickness,

L - the perimeter of the contact area,

θ - the angle between the fragment trajectory and normal to the plate,

a,b – the geometrical sizes of the plate and fragment,

σ_u – ultimate stresses.

Required function for definition of the energy absorbed by a plate:

$$E_{absorbed} = F\,(t, L, \theta, a, b, material) \qquad (1)$$

It is possible to write this equation in the following form:

$$E_{absorbed} = K \cdot f1(t) \cdot f2(L) \cdot f3(\theta) \cdot f4(a,b) \cdot f5(material) \qquad (2)$$

Big engine fragments with kinetic energy up to 150 kJ and small fragments with kinetic energy up to 1 kJ were considered.

2.1 Variation of the Fragment Initial Velocity

Initial velocity of the fragment was varied and residual velocity was determined during parametrical calculations.

Residual velocities of a fragment behind a barrier depending on its initial velocity are shown in Fig. 7, 8. Initial velocity of fragments at which it is braked by barrier are determined (residual velocity is equal to zero).

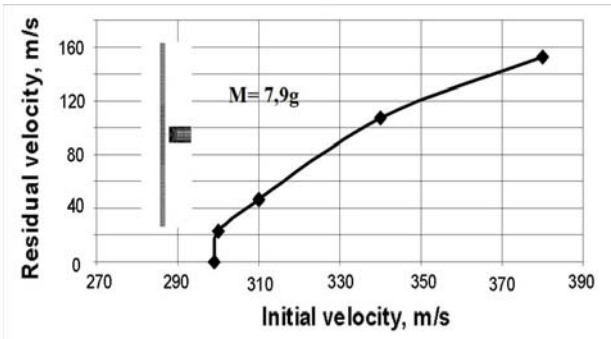

Fig. 7. Residual velocity of the small fragment

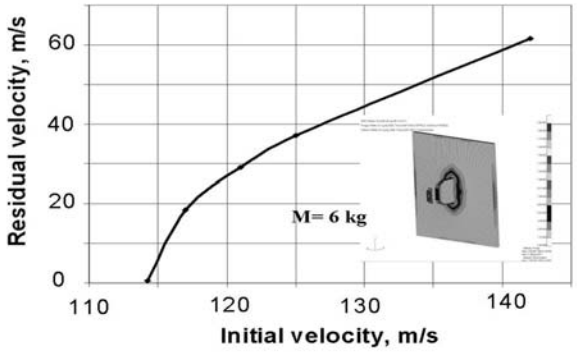

Fig. 8. Residual velocity of the big fragment

The dependences of the fragment kinetic energy before and behind a barrier on a square of the fragment initial velocity are shown in Fig. 9, 10. These dependences have a linear shape.

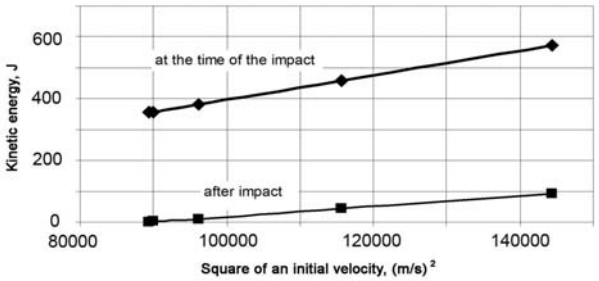

Fig. 9. Kinetic energy of the small fragment

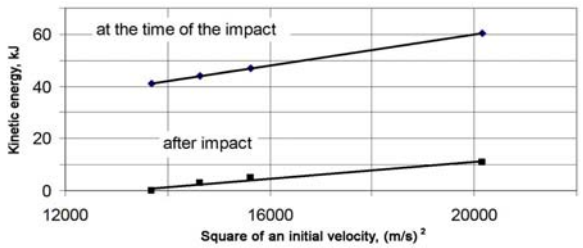

Fig. 10. Kinetic energy of the big fragment

The difference between kinetic energy of a fragment before a barrier and kinetic energy of a fragment after penetrating a barrier is equal to the energy absorbed by a barrier and fragment. The dependences of the absorbed energy on a square of the fragment initial velocity are shown in Fig. 10, 11.

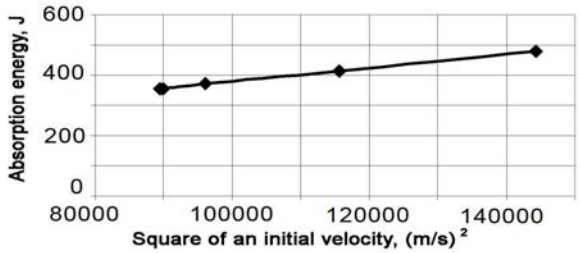

Fig. 11. Absorption energy of small fragment

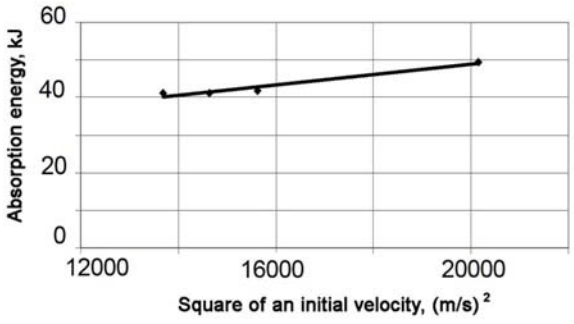

Fig. 12. Absorption energy of big fragment

The absorbed energy by a barrier and fragment grows with increase of the fragment velocity. In a case of the full fragment braking by a barrier (residual velocity of the fragment is equal to zero) absorbed energy has the least value.

2.2 Variation of the Plate Thickness

The results of the variation of a plate thickness *t* are shown in Fig. 13, 14.

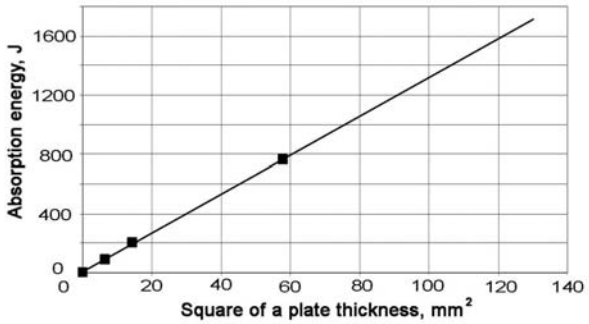

Fig. 13. Influence of the plate thickness (small fragments).

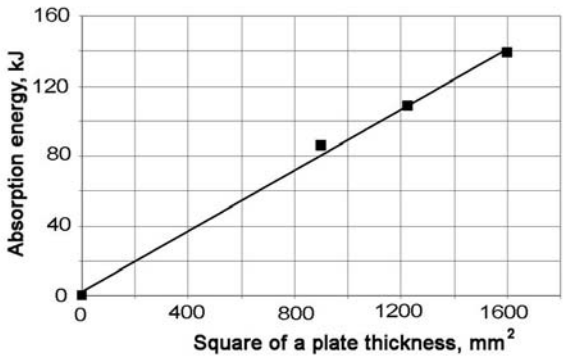

Fig. 14. Influence of the plate thickness (big fragments).

Approximating function of the plate thickness can be written in following form:

$$E_{absorbed} = K \cdot t^2 , \quad f_1(t)=t^2 \qquad (3)$$

2.3 Variation of the Contact Area Perimeter

The results of the variation of a contact area perimeter are shown in Fig. 15, 16.

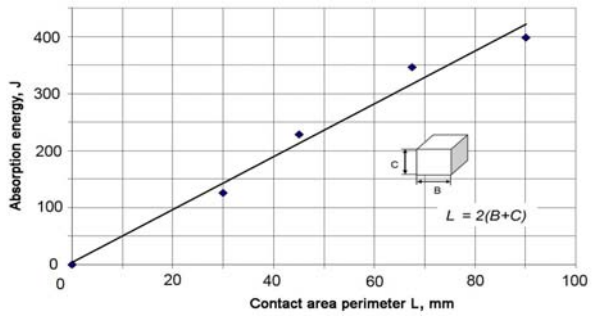

Fig. 15. Influence of the contact area perimeter (small fragments).

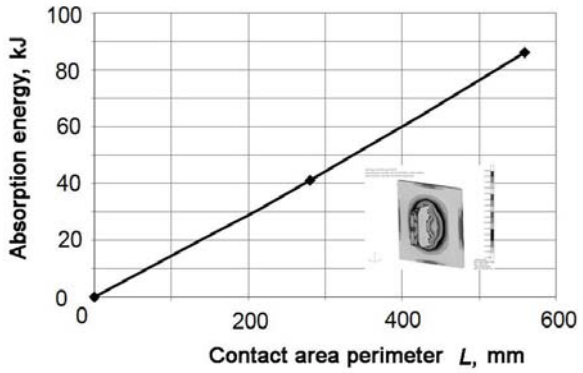

Fig. 16. Influence of the contact area perimeter (big fragments).

Approximating function of the contact area perimeter can be written in following form:

$$E_{absorbed} = K \cdot L, \quad f_2(L)=L \qquad (4)$$

2.4 Variation of the Angle between the Fragment Trajectory and Normal to the Plate

The results of the variation of the angle between the fragment trajectory and normal to the plate are shown in Fig. 17.

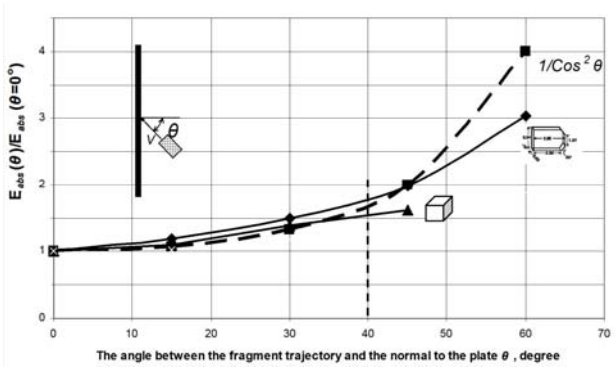

Fig. 17. Influence of the angle between the fragment trajectory and the normal to the plate.

According to this diagram, approximating function of influence of the θ angle in an interval $\theta=0^o$-40^o can be accepted as:

$$E_{absorbed} = K \cdot 1/cos^2\,\theta, \; f_3(\theta)= 1/cos^2\,\theta \qquad (5)$$

At the angles $\theta \geq 40^o$ absorbed energy is much less than the values received with use of approximating function and its value depends on the fragment shape.

2.5 Variation of the Plate Sizes and the Fragment Sizes

The results of the variation of the plate sizes and the fragment sizes are shown in Fig. 18, 19.

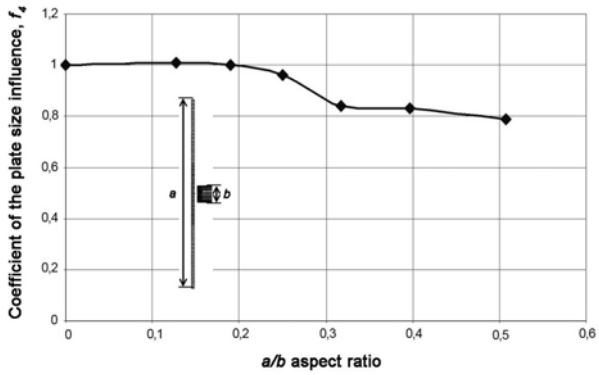

Fig. 18. Influence of the plate sizes and of the fragment sizes (small fragments).

Approximating function of the influence of the plate sizes and of the fragment sizes (small fragments) can be written in following view:

$$f_4(a,b)=1 \text{ under } a/b=0\text{-}0.25 \; ;$$
$$f_4(a,b)=0.8 \text{ under } a/b=0.25\text{-}0.6 \qquad (6)$$

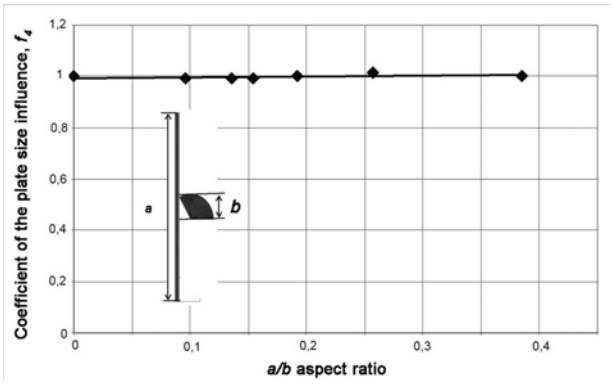

Fig. 19. Influence of the plate sizes and of the fragment sizes (big fragments).

Approximating function of the influence of the plate sizes and of the fragment sizes (big fragments) can be written in following view:

$$f_4(a,b)=1 \qquad (7)$$

2.6 Variation of the Plate Ultimate Stresses

The results of the variation of the plate ultimate stresses are shown in fig. 20. Here the dependence of absorbed energy on value of the

ultimate shear stresses is illustrated. Ultimate shear stresses are determined as $\tau_{sh} = 0{,}6\sigma_u$.

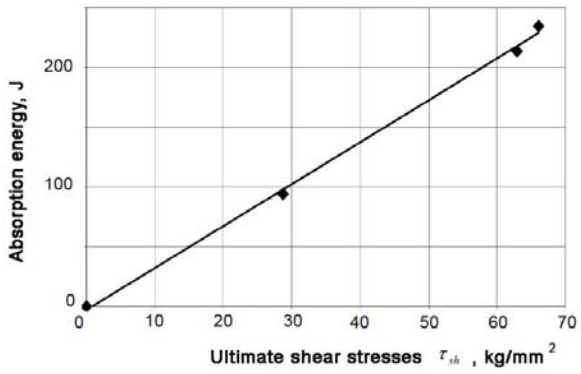

Fig. 20. Influence of the plate ultimate shear stresses.

Approximating function of the influence of the plate ultimate stresses can be written in following form:

$$E_{absorbed} = K \cdot \tau_{sh}, \quad f_5 = \tau_{sh} \tag{8}$$

2.7 Comparison of the Absorbed Energy under Impact of the Deformable and Rigid Fragments

Comparison of the energy absorbed by a plate under impact of the deformable and rigid fragments is shown in Fig. 21.

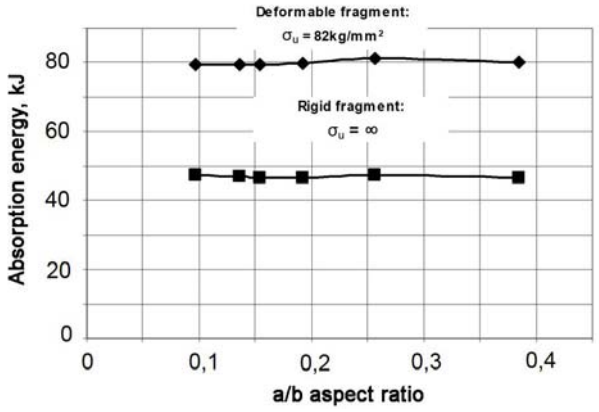

Fig. 21. Comparison of the energy absorbed by a plate under impact of the deformable and rigid fragments

According to Fig. 21 about half of energy it is absorbed due to deformation of a fragment.

2.8 Perforating of the Two Plates

Calculation of two plates perforating by a fragment is performed. The results are shown in Fig. 22. Total absorbed energy for two plates is less than the energy absorbed for one plate with double thickness. Equivalent thickness of a plate is equal to a square root from the sum of squares of thickness for each of the two plates.

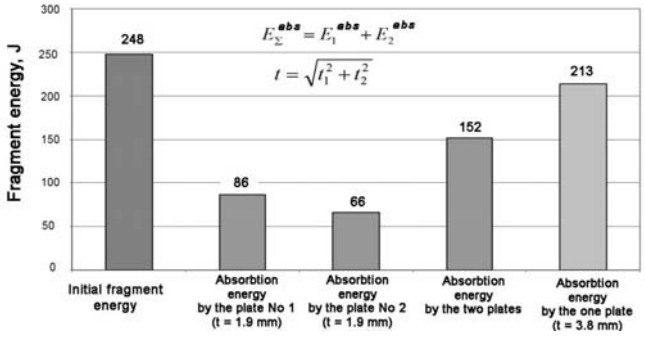

Fig. 22. Perforating of two plates.

4 Summarizing

Summarizing all above mentioned parametrical calculations, the energy absorbed by the plate under the fragment impact can be written down in the following form:

$$E_{absorbed} = K \frac{Lt^2 \tau_{sh}}{Cos^2 \theta} \tag{9}$$

Dependence of coefficient K for the big fragments with high energy is shown in Fig. 23.

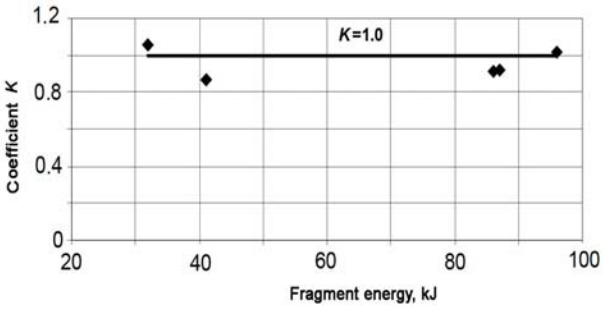

Fig. 23. K coefficient (big fragments).

Dependence of coefficient K for the small fragments is shown in Fig. 24.

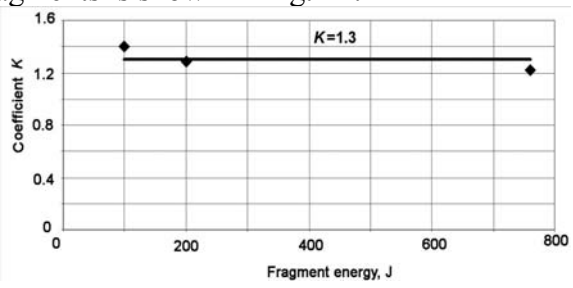

Fig. 24. K coefficient (small fragments).

Thus, the energy absorbed by a plate is determined by the following expression:
for big fragments –

$$E_{absorbed} = \frac{Lt^2 \tau_{sh}}{Cos^2 \theta} \quad (10)$$

for small fragments –

$$E_{absorbed} = 1.3 \frac{Lt^2 \tau_{sh}}{Cos^2 \theta} f(a,b) \quad (11)$$

Here parameters (a and b) are determined from Eqn. 6. Dependences of the absorbed energy on the θ angle are correct only in an interval $\theta = 0^o$-40^o. These empirical dependences can be used in early stages of design for thickness definitions and weight estimations of protective screens.

Conclusions

The engineering method for estimating airframe structure or protective screen energy absorbing under engine debris impact is based on summarizing a lot of numerical parametrical researches in frame of MSC.Dytran code. The MSC.Dytran code verification for the engine fragment impact with kinetic energy 150 kJ is performed by comparison with experiment results. These experiments were conducted in FKP GkNIPAS enterprise field in frame of NACRE program Task 3.2.3. Empirical dependences of the absorbed energy on the engine fragment and plate parameters are received. The comparative analysis of the big engine fragment impact with high energy and small fragments with small energy is conducted. Results of calculation have shown that the energy absorbed by a barrier and fragment grows with increase of the fragment velocity. In case of the full fragment braking by a barrier (residual speed of a fragment is equal to zero) absorbed energy has the least size. This quantity was used at definition of empirical dependences for the absorbed energy. At impact of a plate and a fragment there is their mutual deformation and about half of energy is absorbed due to deformation of a fragment. The engineering method for the analysis of the engine fragment impact will be specified during further numerical and experimental researches at a variation of the greater number of parameters both for fragments and for barriers.

References

[1] National Airlines Albuquerque NTSB Accident Report, NTSB-AAR-75-2 http://case.pr.erau.edu/reports/US_reports/1970/1973.11.03_NationalAirlines_27.pdf.

[2] UAL 232 Sioux City NTSB Accident Report – NTSB/AAR-90-06. http://case.pr.erau.edu/reports/US_reports/1980/1989.07.19_UnitedAirlines_232.pdf

[3] MSC.Dytran, Version 4.0, User manual, 2005.

[4] N.F. Knight Jr, Penetration simulation for uncontained engine debris impact on fuselage-like panels using LS-DYNA, The International Journal of Applied Finite Elements and Computer Aided and Engineering, Volume 36, Number 2, 2000.

[5] Second International Workshop NACRE «New Aircraft Concept Research», 8-11th of July 2008. London Con. Great Britain, DVD. Theses of papers.

Copyright Statement